Journal of Magnetic Resonance 217 (2012) 1–5

Contents lists available at SciVerse ScienceDirect

Journal of Magnetic Resonance

journal homepage: www.elsevier.com/locate/jmr

Perspectives in Magnetic Resonance

Liquid state Dynamic Nuclear Polarization probe with Fabry–Perot resonator at 9.2 T

Vasyl Denysenkov, Thomas Prisner *

Institute for Physical Chemistry, Goethe University Frankfurt, Max von Laue Str. 7, 60438 Frankfurt am Main, Germany

ARTICLE INFO

Article history:
Received 14 November 2011
Revised 23 January 2012
Available online 15 February 2012

Keywords:
Dynamic Nuclear Polarization (DNP)
Electron paramagnetic resonance (EPR)
Nuclear magnetic resonance (NMR)
DNP spectrometer
Double resonance structure
High magnetic fields

ABSTRACT

Recent achievements in liquid state DNP at high magnetic fields showing significant enhancements on aqueous solutions have initiated strong interest in possible applications of this method to biomolecular research. However, *in situ* DNP of biomolecules at ambient temperatures is a challenging task due to high microwave losses leading to excessive sample heating. To avoid such heating the sample volume has to be reduced strongly to keep it away from the electric component of the microwave field. A helical double resonance structure, used for the first demonstrations of the applicability of Overhauser DNP to aqueous solutions at high magnetic fields (9.2 T), restricted the sample size to a very small volume of 2 nl. Together with a poor spectral resolution this resulted in small overall signal amplitude, hampering observations of biomolecules. Here we present a new type of the double resonance structure for liquid-state DNP which consists of a Fabry–Perot resonator for the microwave excitation and a stripline resonator for the NMR detection. This new double resonance structure (260 GHz/400 MHz) offers a 30-fold increase in aqueous sample volume (80 nl) with respect to the helical probe and exhibits improved NMR sensitivity and linewidth.

1. Introduction

The DNP phenomenon, known for more than six decades, has just recently found new applications at high magnetic fields. In most of these applications the polarization transfer is performed on solid state samples, followed by either MAS SS-NMR detection at 90 K [1], or fast dissolution of the sample for room temperature liquid state NMR and MRI [2]. These new experimental methods performed on home-made or commercial setups all rely on solid-state DNP mechanism and found recently widespread applications in material sciences, biomolecular research and imaging [3–10].

In contrary, Overhauser DNP directly performed in the liquid state at high fields has not been developed so intensively due to the following reasons:

(i) Classical Overhauser theory predicts that the DNP enhancement drops significantly with increasing magnetic field. For a typical small paramagnetic molecule, where the translational and rotational correlation times in solution are on the order of 10–20 ps at room temperature, the maximum Overhauser enhancement is achieved for microwave frequencies below 9 GHz, corresponding to magnetic field values below 0.3 T. At higher magnetic fields the enhancement decreases approximately with $1/B^2$ [11];

(ii) High dielectric losses of some solvents in the mm- and submm-wavelength range invoke strong heating of the sample. For example water as solvent for biomolecules exhibits a loss-tangent ≈ 1 at high microwave frequencies. This heating can restrict the microwave (MW) power applied to the sample, hampering saturation of EPR transitions of the radical;

(iii) Powerful enough MW sources, as for example gyrotrons and extended interaction klystrons (EIK), operating in this frequency range became commercially available just now.

For these reasons the development of high field liquid state DNP experimental setups started only recently, demonstrating that significant proton NMR signal enhancements in free-radical containing aqueous solutions can be obtained at high magnetic fields [12–17]. Since liquid state DNP can be employed directly *in situ* on samples under biological conditions, i.e. a liquid water solution, these results are very promising for structural studies of biomolecules in solution. However, the application of such techniques to aqueous solutions at ambient temperatures is a challenging task due to the high dielectric losses in water. This problem can be solved by using a MW resonant structure with the sample placed in a minimum of the electric field of the standing wave. So far the probehead used for *in situ* liquid state DNP consisted of a commercial ENDOR probe developed and optimized for EPR performance [18], an improved version where the MW resonator wall itself serves as an NMR coil [19–21], or an evanescent field resonator where an NMR detection coil is introduced into the sample

* Corresponding author. Fax: +49 (0) 69 79829404.
E-mail address: Prisner@Chemie.Uni-Frankfurt.de (T. Prisner).

1090-7807/$ - see front matter © 2012 Elsevier Inc. All rights reserved.
doi:10.1016/j.jmr.2012.01.014

capillary [22]. All these existing *in situ* DNP probes for liquids can be classified as two fundamental types of resonance structures: a helical/cylindrical double resonance structure; and a dielectric microwave resonance structure with an intra-cavity RF coil.

In the first case the cylindrical body of the EPR cavity is formed by a solenoid radiofrequency (RF) metal tape coil used for NMR excitation and detection. The leads of the coil are connected to a RF circuit tuned to the NMR frequency. A cylindrical TE_{011} microwave mode can be excited in the helix structure by closing the structure on both sides with pistons with a thin metal layer on the top. Such a fundamental mode MW structure has a high MW conversion factor [19,20], but results in very small active sample volumes at higher microwave frequencies. In the second case, the MW resonator is formed by a dielectric tube inserted in a parallel metallic plate structure, following the concept of open non-radiant evanescent field structures. The RF coil is a U-shaped loop with the long axis parallel to the sample capillary, inserted inside the dielectric part of the resonator [22]. Both of these structures are based on fundamental mode MW resonators, restricting the sample size to dimensions far below the MW wavelength. It is possible to increase the sample volume by increasing one index of the TE-mode, i.e. using a higher mode. However, because this only one dimensional extension the gain in sample volume is moderate (for instance, retuning the helix probe from a TE_{011} to a TE_{015} leads to an increase of the sample volume by a factor of 5 only). Also, these types of structures have a poor NMR filling factor and field homogeneity, far from state-of-the-art NMR performances. A further disadvantage is the lack of efficient sample cooling, which strongly restricts the applicable MW power preventing complete saturation of the EPR transitions. Moreover, manufacturing such fundamental mode cavities with high quality factors becomes increasingly difficult at decreasing wavelengths. All these factors are a serious obstacle to apply those probes to biomolecular research.

In the field of EPR Fabry–Perot resonators (FPRs) are being used quite often at frequencies above 90 GHz [23–29]. For example, Freed and coworkers have demonstrated that a FPRs can be used at 250 GHz for EPR on aqueous samples [24]. Furthermore, FPRs have been used for DNP on solid samples [5,34]. This resonator design can handle much larger sample volumes in comparison with single mode cavities. Additionally, they allow a more efficient cooling of the sample, by placing it on the flat mirror of a semi-confocal FPRs and enable higher field homogeneity, because the microwave excitation waveguide (as a source of field inhomogeneity) is more distant from the sample position. The tradeoff is their much lower MW conversion factor; therefore higher microwave excitation power is needed, requiring appropriate sources, e.g. gyrotrons.

In NMR the issue of small sample volumes below one microliter is well investigated [30]. Micro-probes for NMR with microstripes instead of traditional RF coils with high resolution performance have been developed and described in literatures [31,32].

Considering these two aspects in our aim to develop DNP structures with increased sample volumes and improved NMR performance, we have combined a FPRs for the MW excitation with a stripline NMR resonance structure. In this double resonance structure, the stripline is simultaneously used as the flat mirror of the FPRs, with the sample situated on it. In this report we present the electromagnetic (EM) field calculations for this new type of double resonance structure for DNP and ENDOR applications. Additionally, details of the double resonance structure design and optimization, as well as the first experimental tests, demonstrating the excellent performance of the Fabry–Perot stripline probe working at 9.2 T are presented.

2. The double resonance structure design and analysis

The prerequisites for the probe design are: (1) resonance at ω_{NMR} and ω_{EPR} frequencies; (2) homogeneity of the static B_0 field across the sample; (3) reduction of the sample heating.

Taking into account the magnetic field values of modern NMR spectrometers [33], pump frequencies of electron spin transitions can be in the range between 200 GHz and 650 GHz. At these frequencies quasioptical microwave components are preferable. The absorption of microwaves in water reaches 30–100 cm^{-1} at 260 GHz, depending on temperature and salt concentration. Thus, the challenge of operating the DNP probe at 9.2 T, i.e. 260 GHz EPR frequency, is complicated by high dielectric losses in aqueous samples. The influence of the losses can be minimized by applying a resonance structure with well separated E and H components of the MW field, and placing the sample into a node of the E field component (and a maxima of the oscillating B field component). Additionally, an effective heat sink applied to the sample can help to reduce the heating further.

In principle, the heating can also be reduced by substituting CW by pulsed irradiation [34] and by applying circular polarization instead of linear one. However, in this paper we restrict our discussion to items concerning the probe design and performance only.

Among known quasioptical resonators a semiconfocal FPRs with the sample placed on the plain mirror surface (which corresponds to B_{max} and E_{min}) can satisfy the conditions mentioned above. A lumped RF coil in vicinity of the sample, which is placed on top of the plain mirror, could be used as NMR coil; however it will induce Eddy currents in the metal mirror, which deteriorates RF excitation and produces additional sample heating. The use of the flat mirror of the semiconfocal FPRs itself as a stripline NMR resonance structure is the very efficient alternative chosen here and will be described in detail in the following.

2.1. Probe design

The schematic layout of the probe with transversal alignment of the stripline with respect to B_0 is shown in Fig. 1. A semiconfocal FPRs, used for pumping of the EPR transitions at 260 GHz, and a stripline resonator for NMR operation at 392 MHz are combined in this probe design. An implemented version of the double resonance structure is shown in Fig. 3a. A 24 × 5 mm stripe made of 5 μm copper layer deposited on a 0.5 mm quartz substrate is placed inside a 30 × 10 × 5 mm RF shielded box between two parallel copper plates which serve as ground planes of the stripline. The structure contains also tune and match capacitors C_T and C_M shown in Fig. 3a as circular structures attached to the box. There is an opening in one of the shields for the spherical mirror which is positioned in front of the stripe. Thus the stripe is used simultaneously as a plain mirror of the FPRs. Microwave coupling of the FPRs comprises a fundamental TE_{10} mode feed waveguide butted into a recess in the back surface of the spherical mirror. The iris wall thickness of 0.05 mm is chosen as thin as possible. The diameter of the coupling hole was chosen to be 0.4 mm, according to calculations to yield a near-critical coupling for the loaded resonator. The coupling can only be changed by adjusting losses in the cavity, for instance by changing the thickness of the sample. A drop of liquid is placed inside the holder in the shape of a 0.02 mm thin ring of OD = 5 mm/ID = 2.5 mm made of vespel situated on the flat mirror surface. The droplet is then covered with a 0.12 mm quartz cover plate that keeps the sample at the E field node. The proton-free Krytox lubricant (DuPont) has been used for sealing the sample. The cover plate is gently pressed against the holder with an additional spacer ring placed between the quartz cover plate and the upper removable ground plate of the shield box.

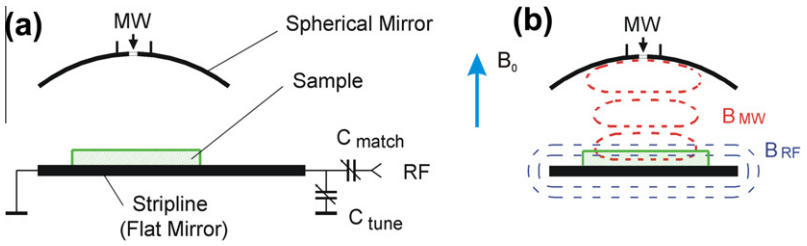

Fig. 1. Schematic layout of the 9.2 T DNP Fabry–Perot-stripline double resonance structure (a); (b) cross section of the structure with a depicted distribution of B_{MW} and B_{RF} field components. Sample plane is orthogonal to B_0 direction.

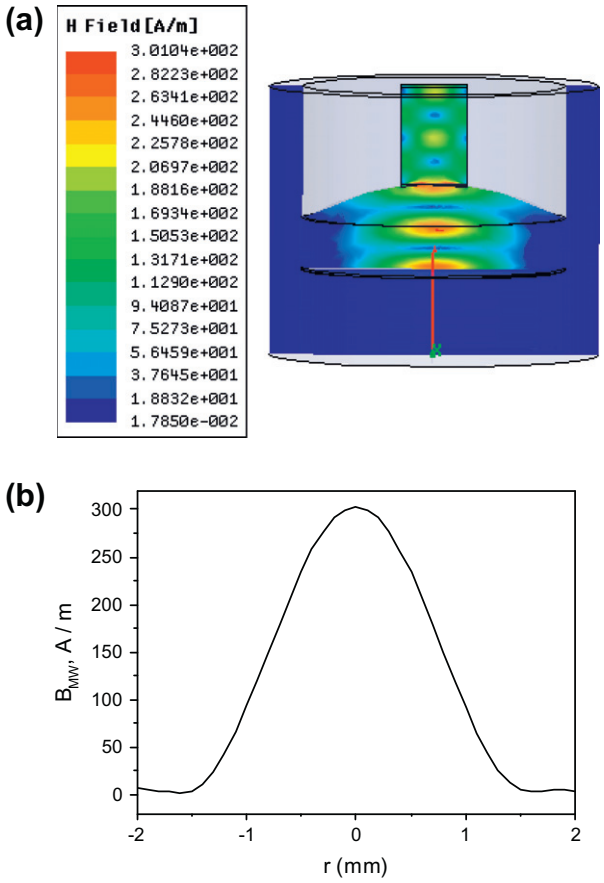

Fig. 2. B_{MW} contour plot diagram across the Fabry–Perot resonator (a) operating in the TEM_{002} mode loaded with an aqueous sample. Diameter of the mirrors is 4 mm, spherical mirror curvature radius is 8 mm, and the mirrors separation is about 1.16 mm. The resonator coupling to the waveguide is achieved by an iris cut into the top of the spherical mirror. The 30 μm thick sample of 3 mm diameter is covered by a 0.12 mm thick quartz plate; (b) calculated field profile along the sample on top of the plain mirror of the Fabry–Perot resonator excited with 1 W of MW power.

2.1.1. Modeling of MW performance at 260 GHz

EM field simulations at 260 GHz were performed using Ansoft HFSSv11 software for a simplified FPRs geometry and an aqueous sample with the following water parameters: $\varepsilon' = 5.6$; $\tan\delta = 1.1$; $\sigma = 1$ S/m. The 30 μm thick water sample is positioned on the flat mirror surface. The resonator with the water sample operating in TEM_{002} mode showed a reasonable loaded Q of 200, versus 700 for the empty resonator. This Q of 700 is far below the typical values for Fabry–Perot resonators at mm-, and sub-mm-wavelengths due to the small dimensions of the spherical mirror and the coupling scheme through the 0.4 mm diameter hole in the centre of the mirror. This leads to significant diffraction and scattering losses, because the iris is a point source for the dipole mode that does not match to the Gaussian mode propagating between mirrors [35]. The probe exhibits a MW conversion factor of about 3.7 G/W$^{1/2}$, which is much lower with respect to the helix cavity (28 G/W$^{1/2}$), as shown in Fig. 2.

2.1.2. Modeling of RF performance at 400 MHz

The simplified geometry of the RF resonance structure including a stripline, a tune capacitor C_T, and a match capacitor C_M, was used as a model to simulate the RF performance of the double resonance structure at 392 MHz (Fig. 3a). A quality factor of 130, and a conversion factor of 25 kHz/W$^{1/2}$ have been calculated from the field distribution (Fig. 3b) and the resonant mode picture (Fig. 3c).

2.1.3. Test results

The double resonance structure has been tested experimentally with our 9.2 T DNP spectrometer [20]. High microwave power was transmitted to the spectrometer from a 20 W gyrotron source (GYCOM; Russia) over the 8 m long corrugated waveguide with total losses of 4 dB resulting in 8 W microwave power at the spectrometer site. MW and RF testing rendered quality factors of $Q_{MW} = 150$ and $Q_{RF} = 100$, respectively, which is slightly below the calculated values due to manufacturing imperfections. DNP and NMR performance of the double resonance structure have been tested for a 24 mM isotopically labelled ^{15}N TEMPOL (Sigma Aldrich) aqueous solution. A 80 nl droplet of the degassed solution was placed within the sample holder. From the nutation experiment (Fig. 4a) the optimal NMR $\pi/2$ pulse has been determined to be 20 μs at 1 W of applied RF power resulting in RF conversion factor $C_{RF} = 10$ kHz/W$^{1/2}$, and the extrapolated ratio of the signal amplitudes after an 810° and a 90° pulse $A_{810}/A_{90} = 0.78$ indicates the RF-homogeneity is similar to commercial liquid-state probes based on saddle-coils that show A_{810}/A_{90} ratio on the order of 80% [32]. A ^{1}H NMR line width of 40 Hz for a water sample has been reached with help of the local shim coils surrounding the sample (Fig. 4b). In contrast to the simulation results, the microwave reflection measurement showed that the probe loaded with the 30 μm of water cannot be coupled efficiently. The critical coupling can be reached experimentally only in the case of a reduced water layer of 20 μm. Some degradation of the MW coupling can be expected due to imminent misalignments of the geometry of the resonator not included in the simulations. During the DNP experiments the low field EPR ^{15}N hyperfine transition was pumped continuously by MW while the NMR free induction decay (FID) of the water protons was recorded. The pulsed NMR repetition time was 3 s, and 4 FIDs were averaged for the signal in Fig. 4c. The peak enhancement of −16 for water protons (Fig. 4c) obtained with 3 W of incident MW power at the resonator is at the moment limited due to a low cooling efficiency. This causes a strong temperature gradient across radial dimensions of the probe, which is difficult to improve within the existing design of the probe.

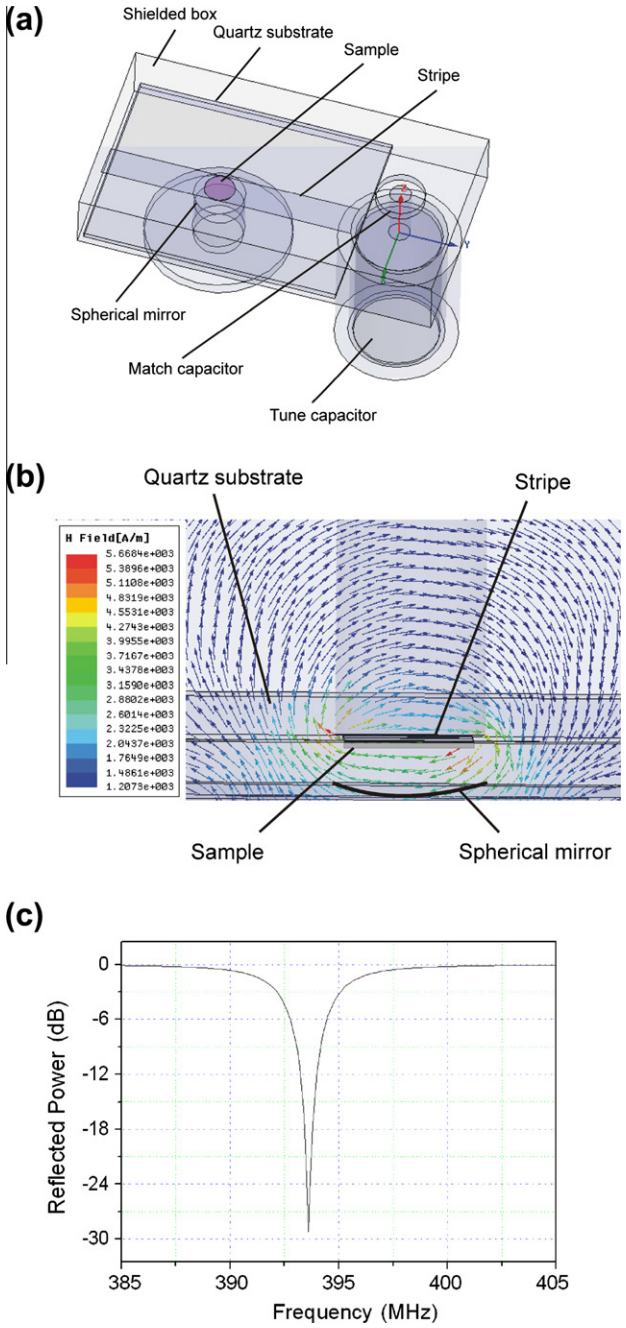

Fig. 3. Geometry used for simulations (a) at 392 MHz with a 5 mm wide and 24 mm long stripline, with the sample (pink) on top of the stripe; (b) vector contour plot showing a magnetic field distribution around the stripline; (c) frequency response of the RF circuit.

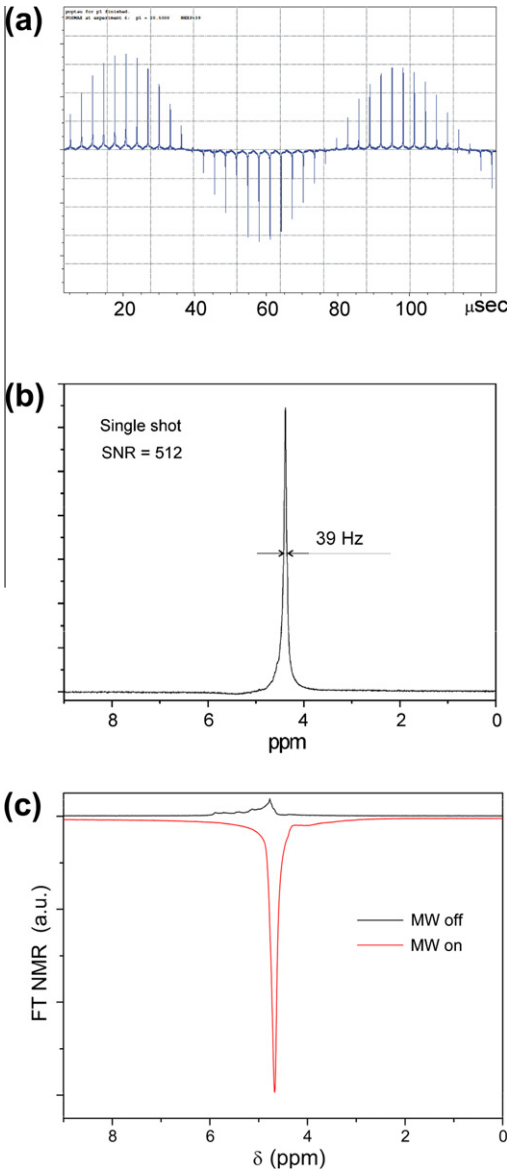

Fig. 4. Experimental test results: (a) proton nutation signal of a deionized water sample at 392 MHz; (b) ^{1}H NMR line of a 320 nl water sample measured by the DRS; (c) DNP enhancement of ^{1}H NMR signal of 24 mM ^{15}N TEMPOL in water solution (4 scans, repetition rate 3 s) for 0.02 mm thick layer sample and 3 mm diameter.

3. Discussion of results

The Fabry–Perot resonator described above was tuned to the TEM_{002} operation mode (Fig. 2a). A separation of the two mirrors equal to the microwave wavelength λ has been chosen here to decrease the radiation losses and to increase the MW power density at the sample. Although the smallest beam waist is accomplished for the confocal separation, it is disadvantageous to operate a resonator at that geometry, because the mode degeneracy can lead easily to mode conversion and therefore higher microwave losses. As mentioned above the resonator has no variable iris, so that the coupling can be changed only by varying sample properties such as thickness and/or loss-tangent (by changing the solvent). In this mode a critical coupling of the resonator has been achieved experimentally with 80 nl of liquid water sample. The B_{MW} field is homogeneous enough across the sample which was restricted to a region smaller that the microwave spot with a Gaussian radial distribution on the flat mirror (Fig. 2). This homogeneity of B_{MW} will be very important for the application of pulsed techniques relying on the phase coherence of the electron spins, as planned for the future.

The DNP enhancement is strongly dependent on the temperature of the sample, which itself depends on the applied MW power. For our measurements we have restricted the microwave power to keep the sample temperature below 310 K to demonstrate the probe performance at temperatures compatible with biological samples, i.e. below 42 °C. Higher enhancements can be obtained with higher microwave power but at elevated sample temperatures. The enhancement at 310 K can be further improved by better sample cooling, planed for the next version of the probe.

In comparison with the helix probe, less lineshape distortions resulting from a temperature gradient over the sample have been observed. Nevertheless, the probe does not show high resolution NMR performance yet (Fig. 4b), due to susceptibility discontinuities along the static field direction in the sample vicinity. The resulting field gradients lead to a proton line of 40 Hz for the water sample. To get high resolution NMR performance, a different design with a longitudinal orientation of the sample with respect to B_0 has to be chosen and all parts surrounding the sample area have to be made of susceptibility-matched construction materials in the shape of thin sections with axial symmetry. This option of the DNP probe is under construction.

The described new double resonance structure might be also useful for HF-ENDOR applications. Especially the high RF conversion factor might be very attractive to achieve short RF π pulses, especially important for low gamma nuclear spins.

4. Conclusions and outlook

The newly developed probe for DNP at 9.2 T allows to use 30-fold enlarged aqueous sample volumes and results in a significantly improved NMR signal sensitivity and linewidth compared to the helix structure. This makes the double resonance structure a promising tool for liquid state biomolecular DNP applications. The achievable DNP enhancement is at the moment still limited by the heat dissipation of the existing probe, which will be improved in the future by applying a heat sink in close vicinity to the sample cooled by nitrogen gas, or water. Further improvement of the spectral resolution of the probe will allow to apply the Overhauser DNP method to biomolecules in the liquid state.

Acknowledgments

We thank Burkhard Endeward, Mark Prandolini, Jan Krummenacker, Petr Neugebauer for fruitful discussions, Marat Gafurov for help with the DNP measurements, Frank Engelke, Alex Krahn and Thorsten Marquardsen from Bruker for technical support to build the probe. Also we express many thanks to Helmut Jäger and Markus van Tankeren from the Institute of Physical Chemistry mechanical workshop for their contribution to the probe construction. We acknowledge the EU Design Study Bio-DNP Project, and the Center for Biomolecular Magnetic Resonance Frankfurt (BMRZ) for financial support of this work.

References

[1] D. Hall, D. Maus, G. Gerfen, S. Inati, L. Becerra, F. Dahlquist, R. Griffin, Polarization-enhanced NMR spectroscopy of biomolecules in frozen solution, Science 276 (1997) 930.
[2] J.H. Ardenkjaer-Larsen, B. Fridlund, A. Gram, G. Hansson, L. Hansson, M.H. Lerche, R. Servin, M. Thaning, K. Golman, Increase in signal-to-noise ratio of >10,000 times in liquid-state NMR, Proc. Natl. Acad. Sci. USA 100 (2003) 10158–10163.
[3] L.R. Becerra, G.J. Gerfen, B.F. Bellew, J.A. Bryant, D.A. Hall, S.J. Inati, R.T. Weber, S. Un, T.F. Prisner, A.E. McDermott, K.W. Fishbein, K.E. Kreischer, R.J. Temkin, D.J. Singel, R.G. Griffin, A spectrometer for dynamic nuclear polarization and electron paramagnetic resonance at high frequencies, J. Magn. Reson. Ser. A 117 (1995) 28–40.
[4] R.A. Wind, R. Hall, A. Jurkiewicz, H. Lock, G. Maciel, Two novel DNP-NMR probes, J. Magn. Reson. 110 (1994) 33–37.
[5] D.J. Singel, H. Seidel, R.D. Kendrick, C.S. Yannoni, A spectrometer for EPR, DNP, and multinuclear high-resolution NMR, J. Magn. Reson. 81 (1989) 145–161.
[6] J. Leggett, R. Hunter, J. Granwehr, R. Panek, A.J. Perez-Linde, A.J. Horsewill, J. McMaster, G. Smith, W. Köckenberger, A dedicated spectrometer for dissolution DNP NMR spectroscopy, Phys. Chem. Chem. Phys. 12 (2010) 5883–5892.
[7] Y. Matsuki, H. Takahashi, K. Ueda, T. Idehara, I. Ogawa, M. Toda, H. Akutsu, T. Fujiwara, Dynamic nuclear polarization experiments at 14.1 T for solid-state NMR, Phys. Chem. Chem. Phys. 12 (2010) 5799–5803.
[8] M. Rosay, L. Tometich, S. Pawsey, R. Bader, R. Schauwecker, M. Blank, P.M. Borchard, S.R. Cauffman, K.L. Felch, R.T. Weber, R.J. Temkin, R.G. Griffin, W.E. Maas, Solid-state dynamic nuclear polarization at 263 GHz: spectrometer design and experimental results, Phys. Chem. Chem. Phys. 12 (2010) 5850–5860.
[9] A. Feintuch, D. Shimon, Y. Hovav, D. Banerjee, I. Kaminker, Y. Lipkin, K. Zibzener, B. Epel, S. Vega, D. Goldfarb, A dynamic nuclear polarization spectrometer at 95 GHz/144 MHz with EPR and NMR excitation and detection capabilities, J. Magn. Reson. 209 (2011) 136–141.
[10] H. Cho, J. Baugh, C.A. Ryan, D.G. Cory, Ch. Ramanathan, Low temperature probe for dynamic nuclear polarization and multiple-pulse solid-state NMR, J. Magn. Reson. 187 (2007) 242–250.
[11] K.N. Hausser, D. Stehlik, Dynamic nuclear polarization in liquids, Advan. Magn. Res. 3 (1968) 79–139.
[12] V.P. Denysenkov, M.J. Prandolini, M. Gafurov, D. Sezer, B. Endeward, T.F. Prisner, Liquid state DNP using a 260 GHz high power gyrotron, Phys. Chem. Chem. Phys. 12 (2010) 5786–5790.
[13] M.J. Prandolini, V.P. Denysenkov, M. Gafurov, B. Endeward, T.F. Prisner, High-field dynamic nuclear polarization in aqueous solutions, J. Am. Chem. Soc. 131 (2009) 6090–6092.
[14] D. Sezer, M.J. Prandolini, T.F. Prisner, Dynamic nuclear polarization coupling factors calculated from molecular dynamics simulations of a nitroxide radical in water, Phys. Chem. Chem. Phys. 11 (2009) 6626–6637.
[15] M.-T. Türke, I. Tkach, M. Reese, P. Höfer, M. Bennati, Optimization of dynamic nuclear polarization experiments in aqueous solution at 15 MHz/9.7 GHz: a comparative study with DNP at 140 MHz/94 GHz, Phys. Chem. Chem. Phys. 12 (2010) 5893–5901.
[16] J.A. Villanueva-Garibay, G. Annino, P.J.M. van Bentum, A.P.M. Kentgens, Pushing the limit of liquid-state dynamic nuclear polarization at high field, Phys. Chem. Chem. Phys. 12 (2010) 5846–5849.
[17] E.V. Kryukov, K.J. Pike, T. Tam, M.E. Newton, M.E. Smith, R. Dupree, Determination of the temperature dependence of the dynamic nuclear polarisation enhancement of water protons at 3.4 T, Phys. Chem. Chem. Phys. 13 (2011) 4372–4380.
[18] P. Hoefer, G. Parigi, C. Luchinat, P. Carl, G. Guthausen, M. Reese, T. Carlomagno, Ch. Griesinger, M. Bennati, Field dependent dynamic nuclear polarization with radicals in aqueous solution, J. Am. Chem. Soc. 130 (2008) 3254–3255.
[19] V. Weis, M. Bennati, M. Rosay, J.A. Bryant, R.G. Griffin, High-field DNP and ENDOR with a novel multiple-frequency resonance structure, J. Magn. Reson. 140 (1999) 293–299.
[20] V.P. Denysenkov, M.J. Prandolini, A. Krahn, M. Gafurov, B. Endeward, T.F. Prisner, High field DNP spectrometer for liquids, Appl. Magn. Reson. 34 (2008) 289–299.
[21] E.V. Kryukov, M.E. Newton, K.J. Pike, D.R. Bolton, R.M. Kowalczyk, A.P. Howes, M.E. Smith, R. Dupree, DNP enhanced NMR using a high-power 94 GHz microwave source: a study of the TEMPOL radical in toluene, Phys. Chem. Chem. Phys. 12 (2010) 5757–5765.
[22] G. Annino, J.A. Villanueva-Garibay, P.J.M. van Bentum, A.A.K. Klaassen, A.P.M. Kentgens, A High-conversion-factor double-resonance structure for high-field dynamic nuclear polarization, Appl. Magn. Reson. 37 (2010) 851–864.
[23] E. Haindl, K. Möbius, H. Ollof, Z. Naturforsch A 40 (1985) 169.
[24] W.B. Lynch, K.A. Earle, J.H. Freed, 1-mm wave ESR spectrometer, Rev. Sci. Instrum. 59 (1988) 1345–1351.
[25] Y.S. Lebedev, in: L. Keven, M. Bowman (Eds.), Modern Pulsed and Continuous-Wave ESR, John Wiley, NY, 1990, p. 365.
[26] H.J. van der Meer, J.A. Disselhorst, J. Allgeler, J. Schmidt, W.Th. Wenckebach, A low-temperature insert for a 95 GHz electron-spin-echo spectrometer, Meas. Sci. Technol. 1 (1990) 396–400.
[27] M. Fuhs, A. Schnegg, T. Prisner, I. Köhne, J. Hanley, A.W. Rutherford, K. Möbius, Orientation selection in photosynthetic PS I multilayers: structural investigation of the charge separated state $P700^+ A_1^-$ by high-field/high-frequency time-resolved EPR at 3.4 T/95 GHz, Biochim. Biophys. Acta 1556 (2002) 81–88.
[28] J. van Tol, L.-C. Brunel, R.J. Wylde, A quasioptical transient electron spin resonance spectrometer operating at 120 and 240 GHz, Rev. Sci. Instrum. 76 (2005) 074101.
[29] P. Neugebauer, A.-L. Barra, New cavity design for broad-band quasi-optical HF–EPR spectroscopy, Appl. Magn. Reson. 37 (2010) 833–843.
[30] M.E. Lacey, R. Subramanian, D.L. Olson, A.G. Webb, J.V. Sweedler, High-resolution NMR spectroscopy of sample volumes from 1 nl to 10 µl, Chem. Rev. 99 (1999) 3133–3152.
[31] P.J.M. van Bentum, J.W.G. Janssen, A.P.M. Kentgens, J. Bart, J.G.E. Gardeniers, Stripline probes for nuclear magnetic resonance, J. Magn. Reson. 189 (2007) 104–113.
[32] J. Bart, J.W.G. Janssen, P.J.M. van Bentum, A.P.M. Kentgens, J.G.E. Gardeniers, Optimization of stripline-based microfluidic chips for high-resolution NMR, J. Magn. Reson. 201 (2009) 175–185.
[33] Bruker Almanac, 2011, pp. 8–20.
[34] S. Un, T. Prisner, R.T. Weber, M.J. Seaman, K.W. Fishbein, A.E. McDermott, D.J. Singe1, R.G. Griffin, Pulsed dynamic nuclear polarization at 5 T, Chem. Phys. Lett. 189 (1992) 54–59.
[35] P. Goy, in: K. Button (Ed.), Infrared and Millimeter Waves, Academic Press, New York, 1976.